Effect of Cholesterol on the Interaction of the HIV GP41 Fusion Peptide with Model Membranes. Importance of the Membrane Dipole Potential[†]

Víctor Buzón and Josep Cladera*

Unitat de Biofísica, Departament de Bioquímica i de Biologia Molecular, i Centre d'Estudis en Biofísica, Facultat de Medicina, Universitat Autònoma de Barcelona, 08193 Bellaterra, Barcelona, Spain

Received March 29, 2006; Revised Manuscript Received September 28, 2006

ABSTRACT: Fusion of viral and cell membranes is a key event in the process by which the human immunodeficiency virus (HIV) enters the target cell. Membrane fusion is facilitated by the interaction of the viral gp41 fusion peptide with the cell membrane. Using synthetic peptides and model membrane systems, it has been established that the sequence of events implies the binding of the peptide to the membrane, followed by a conformational change (transformation of unordered and helical structures into β-aggregates) which precedes lipid mixing. It is known that this process can be influenced by the membrane lipid composition. In the present work we have undertaken a systematic study in order to determine the influence of cholesterol (abundant in the viral membrane) in the sequence of events leading to lipid mixing. Besides its effect on membrane fluidity, cholesterol can affect a less known physical parameter, the membrane dipole potential. Using the dipole potential fluorescent sensor di-8-ANEPPS together with other biophysical techniques, we show that cholesterol increases the affinity of the fusion peptide for the model membranes, and although it lowers the extent of lipid mixing, it increases the mixing rate. The influence of cholesterol on the peptide affinity and the lipid mixing rate are shown to be mainly due to its influence of the membrane dipole potential, whereas the lipid mixing extent and peptide conformational changes seem to be more dependent on other membrane parameters such as membrane fluidity and hydration.

Enveloped viruses employ fusion proteins to enter and infect target cells (*1*, *2*). In HIV-1[1] the fusion protein (glycoprotein gp41) is noncovalently linked to the glycoprotein gp120, forming the so-called envelope (Env) glycoprotein complex (*3*), which seems to be assembled in the viral membrane forming trimers (*4*). The first step in the sequence of events leading to virus entry into the target cell is the binding of gp120 to the CD4 receptor on T-lymphocytes membranes. The interaction of gp120 with members of the chemokine receptor family, acting as coreceptors, is also necessary for successful infection (*5*). Receptor recognition is followed by a structural reorganization of the Env complex, which makes possible the interaction of the amino terminus of gp41 with the target cell membrane (*6*). The amino terminus of gp41 contains the fusion peptide (FP), a 16−23 residue long sequence, highly hydrophobic and rich in glycine and alanine residues (*7*). The interaction of this peptide with the cell membrane is essential for viral and cell membrane fusion to take place since it has been shown that mutations in its sequence completely inhibit the fusion process (*8*−*11*).

The crystal structure of the gp41 ectodomain has been solved, showing that the protein is organized as a trimer (*12*−*14*). However, the protein in the crystals lacks the amino-terminal fusion peptide because of its hydrophobicity. Due to this fact, data on the structure of the peptide and the mechanisms by which the fusion peptide triggers membrane fusion have been obtained using synthetic fusion sequences and model membranes (*15*). These studies have revealed that the fusion process implies the formation of β-pleated structures (*16*−*21*). In a recent study we have shown that the transformation of unordered plus helical structures into β-pleated structures takes place upon membrane binding and precedes lipid mixing (*16*).

Membrane lipid composition is an important factor when considering HIV fusion peptide−membrane interactions. It is well-known that the viral membrane is rich in cholesterol (*22*, *23*), and it seems that budding of the viral particles from the infected cells takes place through the cell membrane microdomains known as rafts (*24*−*26*). The presence of cholesterol in membranes is usually interpreted in terms of its influence on membrane fluidity. But cholesterol, as a molecular dipole, can influence another, less known, physical parameter in the lipid bilayer: the membrane dipole potential. In the past few years the influence of the dipole potential on several biological systems has been reported (*27*−*35*).

[†] This work was funded by the Fundació La Marató de TV3, Grant 020410 to J.C.

* Corresponding author. E-mail: josep.cladera@uab.cat. Phone: 00-34-935812112. Fax: 00-34-935811907.

[1] Abbreviations: HIV-1, human immunodeficiency virus type 1; PC, egg phosphatidylcholine; PE, egg phosphatidylethanolamine; CHOL, cholesterol; 6-KC, 6-ketocholestanol; DMSO, dimethyl sulfoxide; FPE, fluorescein−phosphatidylethanolamine; Rh-PE, *N*-(lissamine rhodamine B sulfonyl)phosphatidylethanolamine; NBD-PE, *N*-(nitrobenz-2-oxa-1,3-diazolyl)phosphatidylethanolamine; di-8-ANEPPS, 1-(3-sulfonatopropyl)-4-[β-[2-(di-*n*-octylamino)-6-naphthyl]vinyl]pyridinium betaine; FP, fusion peptide; LUVs, large unilamelar vesicles; FTIR, Fourier transform infrared; gp41, glycoprotein 41; gp120, glycoprotein 120; FRET, fluorescence resonance energy transfer.

10.1021/bi060622i CCC: $33.50
Published on Web 12/01/2006

This membrane potential is generated by the presence of electrical dipoles on the phospholipid molecules and the presence of oriented water molecules at the membrane−water interface (*36*). In the case of viral fusion peptides there is some scarce evidence that the magnitude of the membrane dipole potential can affect the extent of the fusion process (*37*). The magnitude of the membrane dipole potential can be modulated in model membranes using, besides cholesterol, other sterols, such as 6-ketocholestanol and phloretin (*38*, *39*).

In the present work we have studied how cholesterol and 6-ketocholestanol affect the interaction of a 23 residue long HIV fusion peptide with model membranes and which events leading to membrane fusion (binding to the membranes, conformational changes, and lipid mixing) can be related to changes in the magnitude of the dipole potential. The approach based on the combined use of fluorescence and infrared spectroscopies shows that the interaction of the fusion peptide with model membranes is affected by the magnitude of the membrane dipole potential. The affinity of the fusion peptide is higher for model membranes with higher values of the dipole potential (more positive toward the center of the membrane). Increasing the magnitude of the dipole potential increases as well the lipid mixing rate. Variations on the extent of the conformational changes associated to membrane binding and fusion and lipid mixing extent are, however, shown to be dependent upon other membrane properties such as the membrane fluidity and membrane hydration.

MATERIALS AND METHODS

Materials. Egg phosphatidylcholine (PC) and phosphatidylethanolamine (PE) were purchased from Avanti Polar Lipids. Cholesterol (CHOL), 6-ketocholestanol (6-KC), and reduced Triton X-100 were purchased from Sigma. Fluorescein−phosphatidylethanolamine (FPE), *N*-(lissamine rhodamine B sulfonyl)phosphatidylethanolamine (Rh-PE), *N*-(nitrobenz-2-oxa-1,3-diazolyl)phosphatidylethanolamine (NBD-PE), and 1-(3-sulfonatopropyl)-4-[*β*-[2-(di-*n*-octylamino)-6-naphthyl]vinyl]pyridinium betaine (di-8-ANEPPS) were purchased from Molecular Probes. Deuterated dimethyl sulfoxide (DMSO) (spectroscopy grade) was purchased from Merck. All other reagents were of analytical grade.

Peptide Synthesis. The sequence corresponding to the N-terminus of the HIV-1 gp41 protein was synthesized using chloride as a counterion and purified (estimated homogeneity >90%) by Jerini Peptide Technologies (Berlin, Germany). Peptide stock solutions were prepared in deuterated dimethyl sulfoxide. The sequence for FP23H was H-AVGIGALFLG-FLGAAGSTMGARS-$CONH_2$.

Preparation of Large Unilamellar Vesicles (LUVs). Large unilamelar lipid vesicles were prepared according to Mayer et al. (*40*). Phosphatidylcholine, phosphatidylethanolamine, and cholesterol (all in chloroform) or 6-ketocholestanol (in methanol), when required, were mixed in a round-bottom flask and dried under a stream of nitrogen gas by rotary evaporation until a thin film of lipids was formed. The film was resuspended in buffer (10 mM Tris, pH 7.5, for fluorescence experiments or 10 mM HEPES, pD 7.5, for infrared measurements) and then frozen and thawed five times. Finally, the vesicle suspension was extruded 10 times through two polycarbonate filters of pore size 100 nm using a Liposofast extruder. Liposomes were always 100 nm in diameter according to control measurements carried out with a Ultrafine particle analyzer (data not shown).

Labeling of LUVs with FPE and Di-8-ANEPPS. LUVs were labeled exclusively in the outer bilayer leaflet with the surface potential sensor fluorescein−phosphatidylethanolamine (FPE) as described (*16*). Briefly, the unilamellar vesicles were incubated with FPE dissolved in ethanol (never more than 0.1% of the total aqueous volume) at 37 °C for 1 h in the dark. Any remaining unincorporated FPE was removed by gel filtration on a PD10 Sephadex G-25 column (Amersham Biosciences) equilibrated with the appropriate buffer. Such a procedure leads to the incorporation of 30−50% of the externally added FPE to the preformed membrane vesicle. Furthermore, there was no observed transmembrane flipping of the FPE, at least over time scales of 1 week. The FPE liposomes were stored at 4 °C until use.

LUVs were labeled with the dipole potential fluorescent sensor di-8-ANEPPS [1-(3-sulfonatopropyl)-4-[*β*-[2-(di-*n*-octylamino)-6-naphthyl]vinyl]pyridinium betaine] by adding the dye at a final concentration of 8 μM (from a stock solution in ethanol) into a cuvette containing LUVs at a final concentration of 300 μM. LUVs were incubated overnight at 37 °C in the dark with the dye to ensure its complete labeling.

Fluorescence Measurements with FPE-Labeled Membranes. Fluorescence time courses of FPE-labeled vesicles were measured after adding the desired amount of peptide into 2 mL of lipid suspensions (300 μM lipid) with a SLM-Aminco 8000 spectrofluorometer. Excitation and emission wavelengths were set at 490 and 520 nm, respectively. Temperature was controlled with a thermostatic bath at 20 °C. The contribution of light scattering to the fluorescence signals was measured in experiments without the dye and was subtracted from the fluorescence traces. Data were fitted to a sigmoidal binding model (*41*) using the equation:

$$F = (F_{max}[FP])^n/(K_d^n + [FP])^n \quad (1)$$

where F is the fluorescence variation, F_{max} the maximum fluorescence variation, [FP] the fusion peptide concentration, K_d the dissociation constant of the membrane binding process, and n the Hill coefficient. The experimental points shown in the figures are the mean value of two measurements. In experiments with FPE-labeled membranes with membranes supplemented with 6-KC or cholesterol, particular attention was paid to the fact that the initial fluorescence level was the same as for the control membranes (PC/PE membranes) in order to have an indication that the additives were not affecting the magnitude of the surface potential (membrane surface electronegativity).

Fluorescence Measurements with Di-8-ANEPPS-Labeled Membranes. Di-8-ANEPPS excitation spectra were obtained by exciting the vesicle suspension at 460 nm and collecting their emission at 580 nm. Dual-wavelength recordings with the di-8-ANEPPS dye were obtained by exciting the samples at two different wavelengths (430 and 510 nm) and measuring their emission intensity ratio, $R_{430/510}$, at 580 nm (*42*, *43*). Any contribution of light scattering to the fluorescence signals was corrected from identical recordings with unla-

beled membranes. Temperature was controlled with a thermostatic bath at 20 °C.

Lipid Mixing Measurements. Lipid mixing experiments were carried out by measuring the fluorescence intensity change resulting from the fluorescence resonance energy transfer (FRET) between NBD-PE and Rh-PE, inserted into the lipid bilayer, as described by Struck et al. (*44*). Fluorescence was monitored by using an SLM-Aminco 8000 spectrofluorometer. Vesicles were prepared as described above except that the dyes were added into the initial organic lipid solution. Vesicles containing both dyes at 0.6 mol % each were mixed with dye-free vesicles (1:9 molar ratio) at a final lipid concentration of 300 μM. The initial fluorescence of the labeled/unlabeled vesicle suspension was taken as 0% lipid mixing, and the 100% lipid mixing was determined by adding reduced (to eliminate quenching of the NBD probe) Triton X-100 at a final concentration of 0.1% (v/v). The excitation wavelength was 465 nm and emission wavelength 530 nm. Temperature was controlled with a thermostatic bath at 20 °C. The experimental points shown in the figures are the mean value of two measurements. In all cases particular attention was paid to the initial level of fluorescence in lipid mixing experiments in order to ensure that the intial fluorescence was the same for the different membrane compositions. This allowed us to rule out any lipid mixing previous to the one due to the peptide, coming from, for example, the presence of cholesterol in the bilayer.

Fourier-Transform Infrared Spectroscopy (FTIR) Measurements. FTIR spectra were recorded at 20 °C on a FTIR-Mattson Polaris spectrometer, equipped with a cooled nitrogen−cadmium−telluride (MCT) detector, at a nominal resolution of 2 cm^{-1}. The spectrometer was continuously purged with dry air (dew point lower than −60 °C). The spectra were corrected for atmospheric water vapor contribution. For time-resolved experiments vesicles from stock solutions in deuterated buffer and the FP23H peptide from a stock solution in DMSO were mixed to give a lipid-to-peptide ratio of 10 and immediately placed between two CaF_2 windows separated with a 50 μm spacer. Twenty scans were collected and averaged using a shuttle device every 110 s for 1 h. The concentration of the lipid vesicles was kept around 10 mM and the concentration of FP23H around 1 mM.

For the analysis of the carbonyl lipid band, 500 spectra were collected and averaged using a shuttle device. The lipid concentration was 10 mM. Spectra were corrected for solvent contribution. Component band curve fittings were carried out using the program Grams (Galactic Inc.).

RESULTS

Modulation of LUVs' Membrane Dipole Potential by Cholesterol and 6-Ketocholestanol. Variations in the magnitude of the membrane dipole potential can be monitored using the fluorescent sensor di-8-ANEPPS. Changes in the total membrane dipole moment are known to cause a shift in the excitation spectrum maximum of the dye, which is usually measured as an excitation difference spectrum. In agreement with previous reports (*45*), the difference excitation spectra shown in Figure 1A reveal that both cholesterol and 6-ketocholestanol increase the magnitude of the membrane dipole potential in PC/PE membranes. The maximum

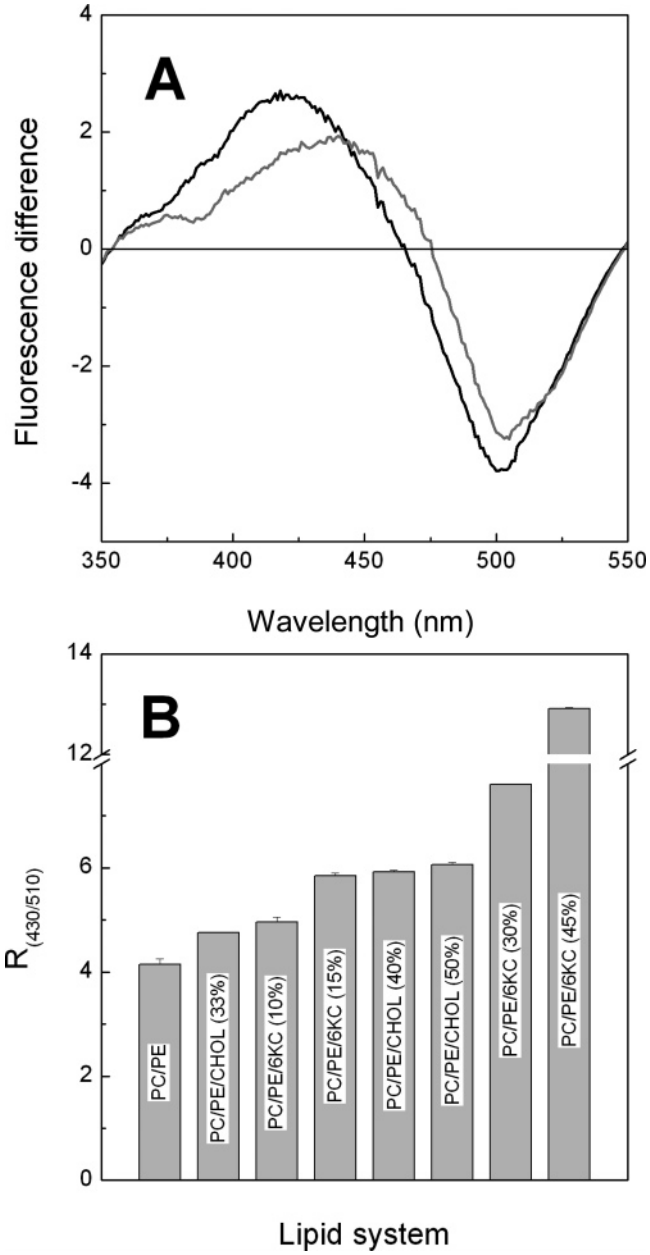

FIGURE 1: (A) Difference in excitation spectra (emission 580 nm) for di-8-ANEPPS-labeled PC/PE vesicles containing 15 mol % 6-KC (gray line) or 50 mol % CHOL (black line) subtracted from labeled vesicles containing no additive. (B) Dependence of the magnitude of the dipole potential, expressed as the fluorescence ratio $R_{430/510}$, on membrane composition. The mol % of CHOL or 6-KC is indicated in parentheses.

around 430−450 nm and the minimum around 510 nm are a consequence of the blue shift caused in the excitation spectra of di-8-ANEPPS when the dipole potential is made more positive toward the center of the bilayer. By exciting the membrane suspensions at the two different wavelengths corresponding to the maximum and the minimum of the difference spectrum, a fluorescence intensity ratio *R* can be calculated. This ratio can be used as a measure of the relative changes in the magnitude of the dipole potential: the higher the *R* the more positive the dipole potential toward the center of the bilayer (*38*, *43*, *46*). In Figure 1B the values of the fluorescence intensity ratio *R* as a function of the different membrane compositions used throughout the present work are shown.

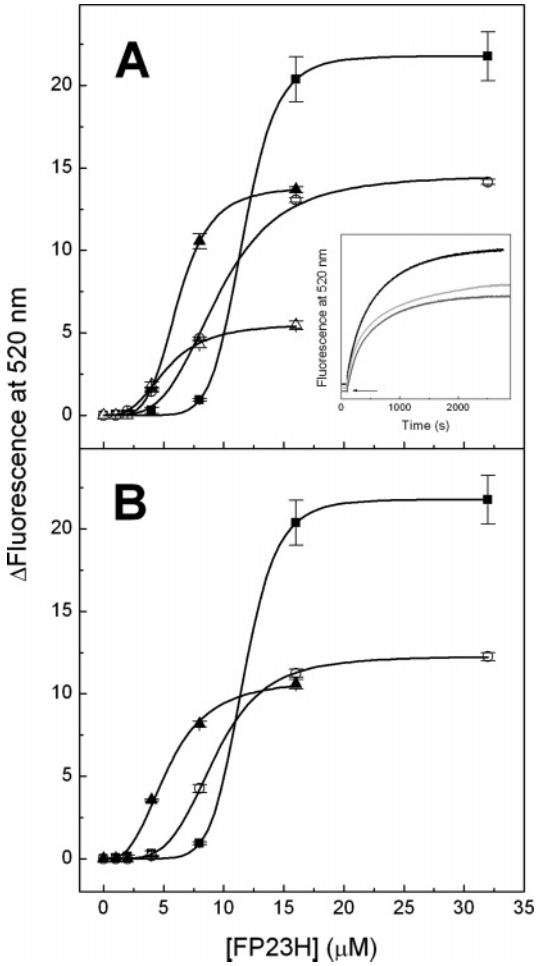

FIGURE 2: Binding of the fusion peptide to FPE-labeled vesicles. The binding curves were derived from the time course fluorescence variations caused by addition of FP23H to PC/PE FPE-labeled membranes [panel A inset: addition of FP23H at a final concentration of 30 μM to PC/PE FPE-labeled membranes (black line), with 30 mol % 6-KC (light gray line) and with 33 mol % CHOL (gray line), indicated by the arrow. The initial fluorescence level is the same, within experimental variation, for the different membrane compostions; this means that addition of either cholesterol or 6-KC does not affect the magnitude of the surface potential]. (A) PC/PE membranes containing 0 mol % 6-KC (filled squares), 10 mol % 6-KC (open circles), 15 mol % 6-KC (filled triangles), and 30 mol % 6-KC (open triangles). (B) PC/PE membranes containing 0 mol % CHOL (filled squares), 33 mol % CHOL (open circles), and 40 mol % CHOL (filled triangles). PC and PE were always equimolar in the model membranes. The lipid concentration was 300 μM. The temperature was 20 °C. The buffer was 10 mM Tris, pH 7.5. The solid line represents the best fits using eq 1. Each data point in the binidng curve is the mean value of two independent determinations (two independent binding curves), and the error bars correspond to the range of the mean.

Effect of Cholesterol and 6-Ketocholestanol on the Binding of the Fusion Peptide to PC/PE Model Membranes. Binding of the fusion peptide to model membranes was monitored using the fluorescent probe fluorescein−phosphatidylethanolamine (FPE), which is sensitive to changes in the electrostatic surface potential (*41*). The interaction of the positively charged peptide with the membrane resulted in an increase of the fluorescence intensity of FPE, as shown in Figure 2A (inset), which is consistent with an increase in the electropositivity of the surface potential. The cumulative changes of fluorescence intensity represented as a function of peptide concentration (binding curves) are shown in Figure

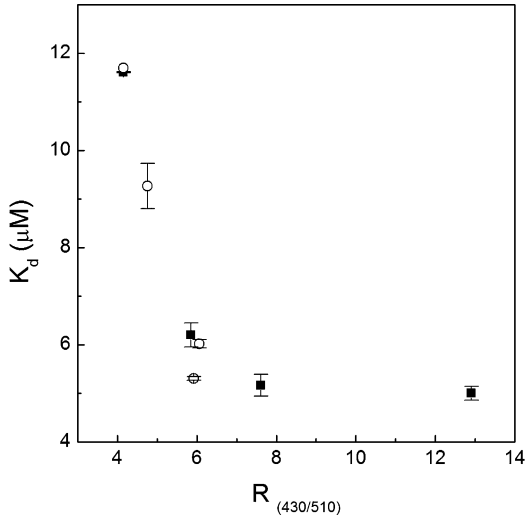

FIGURE 3: Fluorescence ratio $R = I_{430}/I_{510}$ as a function of the dissociation constants derived from Figure 2. Different percentages of 6-KC (filled squares) and CHOL (open circles) in the membranes have been converted into the corresponding R value using Figure 1B. K_d values have been calculated as the mean value from two independent fittings to eq 1 of the two experimental binding curves available (see Figure 2 legend) for each membrane composition. Errors bars are the range of the mean. Fitting of the experimental points to eq 1 was highly reproducible: the regression coefficient was $R = 0.99$ in all cases, and the mathematical (fitting) errors in the calculation of the dissociation constant from the fittings were as in the following examples: K_d(PC/PE) = 11.6 ± 0.2; K_d(10% KC) = 9.5 ± 0.61; K_d(15% KC) = 6.2 ± 0.02; K_d(30% KC) = 5.2 ± 0.32; K_d (33% chol) = 9.24 ± 0.06; K_d(40% chol) = 5.3 ± 0.4.

2A (effect of 6-ketocholestanol) and Figure 2B (effect of cholesterol). In all cases the binding data fit eq 1, a sigmoid which can imply some degree of cooperativity in the binding process (*41*). One interpretation of this cooperativity is that perhaps the initial membrane contacts involve interactions between more than one peptide molecules (the number of peptide molecules involved would be given by the Hill coefficient, n) (*41*). Nevertheless, it is not possible to simply establish a direct link between this cooperativity and the known formation of gp41 oligomers on the viral and cell membranes (see ref *16*). The clear differences observed in the fluorescence intensities reached at the plateaus, depending on the membrane sterol content, correspond to different degrees of surface potential disturbance caused by peptide binding. These differences could be due to a difference in the membrane binding capacity (number of peptide molecules bound per lipid molecule) although differences in the conformation of the bound peptides could also contribute to the observed fluorescence changes. On the other hand, the binding curves reveal an unequivocal effect of the sterol content on the affinity of the peptide for the membrane. Both cholesterol and 6-ketocholestanol cause a decrease in the value of the dissociation constant calculated using eq 1 (Figure 3). This increase in the affinity of the peptide for the membrane must be due to the increase in the magnitude of the dipole potential caused by the two sterols, since they have an opposite effect on other physicochemical parameters, such as hydration or fluidity (see Discussion).

Effect of Cholesterol and 6-Ketocholestanol on Membrane Lipid Mixing. The peptide fusogenic capacity was monitored by measuring its ability to induce lipid mixing between model membranes composed of PC/PE (1:1) alone or supplemented

with 6-ketocholestanol or cholesterol. The NBD fluorescence increase (decrease in energy transfer) as a consequence of the lipid mixing caused by the addition of the peptide for different membrane lipid compositions at a lipid/peptide ratio of 10 is shown in Figure 4A,B. It can be deduced from this figure that 6-ketocholestanol increases both the rate and the extension of lipid mixing whereas the presence of cholesterol reduces the extent of lipid mixing, and its influence on the mixing rate depends on the cholesterol molar percentage in the membrane. From these data a different influence of the dipole potential (mainly affecting the lipid mixing rate) and of the fluidity and/or hydration of the membrane (mainly affecting the lipid mixing extent) can be deduced (see Discussion). The different effect of cholesterol and 6-ketocholestanol on the lipid mixing extent is also apparent from Figure 4C (maximum lipid extent is given by the percentages at the plateaus), where the lipid mixing percentage has been plotted as a function of peptide concentration. Comparison of the curves plotted in Figure 4C with the binding curves shown in Figure 2 reveals that fusion takes place as binding occurs. In fact, similar values of the dissociation constant were obtained when fitting the data in Figure 4C to eq 1, compared to those derived from Figure 2.

Effect of Cholesterol and 6-Ketocholestanol on the Fusion Peptide Conformation upon Interaction with the Membrane. In order to gain insight on the structural changes taking place during the interaction of the fusion peptide with membranes, we monitored the secondary structure variations of FP23H as a function of time, in the absence and the presence of membranes of different lipid composition. The FTIR spectra obtained at a fusogenic lipid/peptide ratio are shown in Figure 5 and are in general dominated by two main features: a band with a maximum at 1624 cm^{-1}, characteristic of aggregated intermolecular β-structures, and another band with a maximum centered around 1648 cm^{-1}, which corresponds to a mixture of unordered and helical structures (*47*). The dilution of the peptide in aqueous buffer and the interaction with model membranes implies the transformation of unordered plus helical structures into β-aggregated structures. These transformations become more apparent if we represent the ratio Abs_{1624}/Abs_{1648} as a function of time (Figure 6). According to the data and in agreement with previous reports (*16*) the presence of membranes favors the transformation of unordered plus helical structures into β-sheet aggregates. Cholesterol up to 50% does not affect much the amount of structures converted into β-sheet, a conversion which is, however, clearly enhanced by the presence of 15 mol % 6-ketocholestanol. Since 50 mol % cholesterol and 15 mol % 6-ketocholestanol cause a similar increase in the magnitude of the dipole potential of PC/PE membranes (see Figure 1B), the observed effect on the formation of β-structures would rather be caused by the increase in membrane fluidity and/or hydration due to the presence of 6-ketocholestanol, rather than to the variation of the dipole potential.

Effect of Cholesterol and 6-Ketocholestanol on Lipid Hydration. Since it has been previously established that the interaction of the 23 residue long HIV fusion peptide with model membranes causes a dehydration of the lipid−water interface (*16*, *19*), we have measured how the presence of cholesterol or 6-ketocholestanol affects the hydration degree of the model membranes used in the present study. Figure 7 shows the phospholipid carbonyl region of the infrared

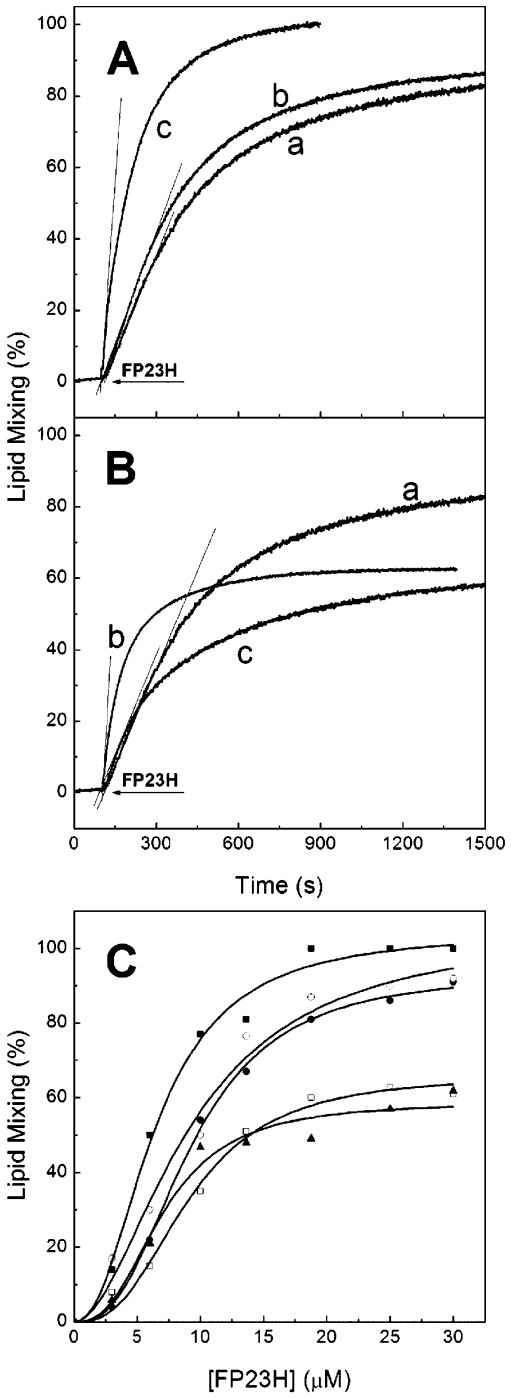

FIGURE 4: Lipid mixing time course induced by addition of FP23H (at a final 30 μM final concentration) to membrane suspensions supplemented either with 6-KC or with CHOL. (A) (a) PC/PE, (b) PC/PE and 15 mol % 6-KC, and (c) PC/PE and 30 mol % 6-KC; (B) (a) PC/PE, (b) PC/PE and 33 mol % CHOL, and (c) PC/PE and 50 mol % CHOL. (C) Percentage of lipid mixing induced by addition of FP23H to NBD/Rh-labeled membranes as a function of peptide concentration. The membrane composition was as follows: PC/PE (solid circles); PC/PE and 15 mol % 6-KC (open circles); PC/PE and 30 mol % 6-KC (solid squares); PC/PE and 40 mol % CHOL (open squares); PC/PE and 50 mol % CHOL (solid triangles). PC and PE were equimolar in all model membranes. The lipid concentration was 300 μM. The temperature was 20 °C. The buffer was 10 mM Tris, pH 7.5. During lipid mixing experiments samples were coninuously and gently stirred using a magnetic stirrer. The solid line represents the best fits using eq 1. Gray straight lines are drawn in order to help appreciating the differences in the initial lipid mixing rate for the different membrane compositions.

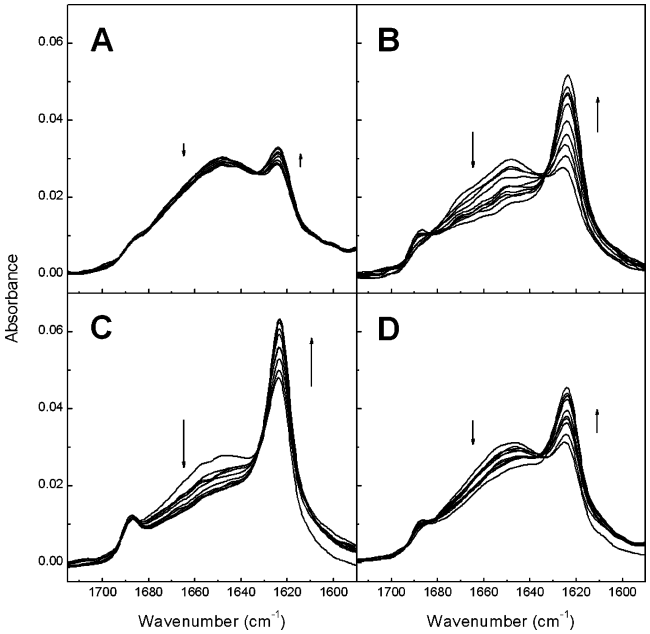

FIGURE 5: Fourier transform infrared (FTIR) spectra of the FP23H peptide (1 mM) in deuterated 10 mM HEPES buffer (A) and mixed with membrane suspensions (10 mM lipid) with the following compositions: (B) PC/PE; (C) PC/PE and 15 mol % 6-KC; (D) PC/PE and 50 mol % CHOL. Spectra were acquired as a function of time. Each spectrum is the average of 20 scans, and the spectral contribution of the buffer was always subtracted. One spectrum was collected every 110 s. The temperature was 20 °C. The buffer was 10 mM HEPES, pD 7.5. The series of spectra shown are representative of two independent measurements. Arrows indicate spectral regions where the intensity increases (↑) and decreases (↓).

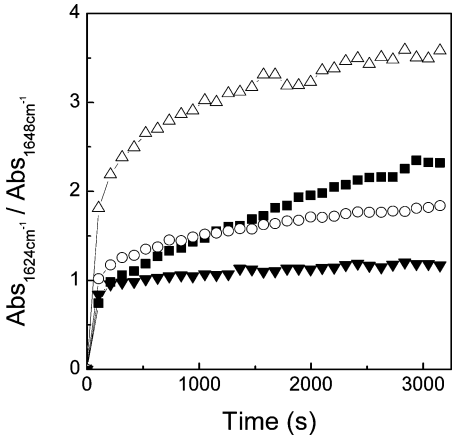

FIGURE 6: Kinetics of the structural changes illustrated in Figure 5. The transformation of helical + unordered structures into β-aggregates has been plotted as the ratio Abs_{1624}/Abs_{1648} versus time: PC/PE vesicles (filled squares); PC/PE vesicles with 15 mol % 6-KC (up open triangles), PC/PE vesicles with 50 mol % CHOL (open circles); FP23H into buffer (down filled triangles). Each data point is the average of two independent experiments.

spectra of PC/PE membranes containing different molar percentages of either cholesterol or 6-ketocholestanol. Three infrared bands are detected: one centered around 1739−1744 cm^{-1}, which can be assigned to the stretching vibration of the dehydrated phospholipid carbonyls; another one centered around 1720−1730 cm^{-1}, assignable to phospholipid carbonyls which are hydrogen bonded to water molecules; and a third band around 1710 cm^{-1} which corresponds to bihydrated carbonyl groups (*48*, *49*). It is clear from Figure 7 that 6-ketocholestanol reduces the percentage

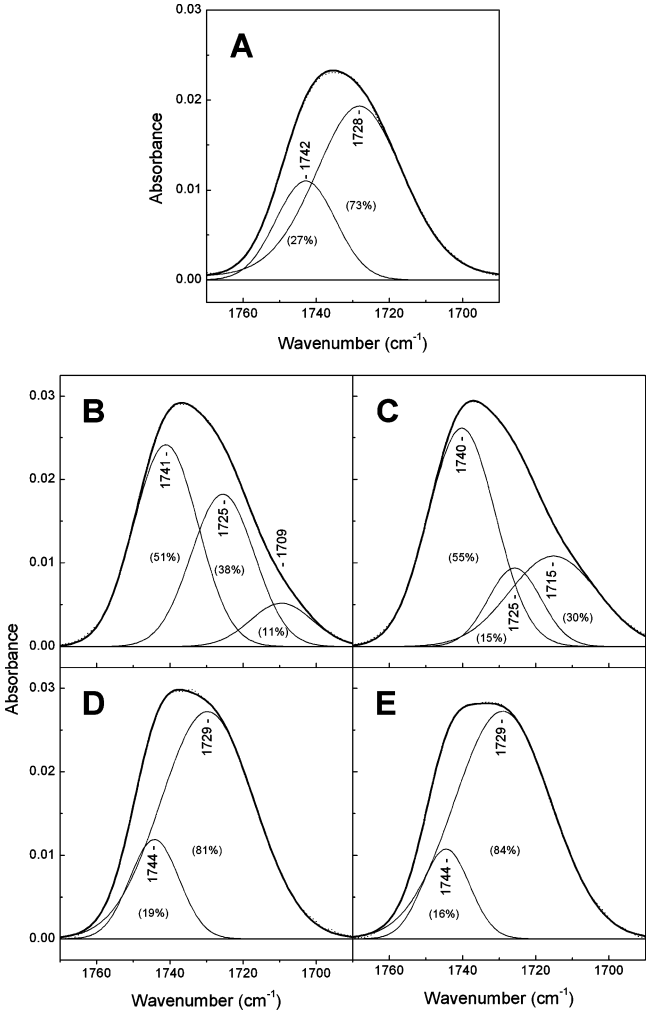

FIGURE 7: Ester carbonyl region of the FTIR spectra of (A) PC/PE (1:1) model membranes, (B) PC/PE with 15 mol % of 6-KC, (C) PC/PE with 30 mol % 6-KC, (D) PC/PE with 33 mol % CHOL, and (E) PC/PE with 50 mol % CHOL. Component bands were fitted to the original spectra using Grams 3.2 (Galactic Inc.). Numbers in parentheses indicate the percentage of the total carbonyl band corresponding to each component.

of ester carbonyls hydrogen bonded to water molecules whereas cholesterol increases the hydration of the lipid headgroups. In all cases, addition of the peptide to the membranes did cause a reduction in the level of hydration (data not shown) in agreement with previous observations (*16*).

DISCUSSION

Cholesterol is an important component of the HIV envelope membrane, where the cholesterol/phospholipid ratio is around 0.9 (*22*, *23*). It has been described that the use in vitro of fluidizing agents, acting on the membrane cholesterol content, reduces HIV infection and replication (*50*−*52*). The relationship between cholesterol and membrane fluidity has been widely studied. Cholesterol, however, is a molecule bearing a dipole moment, and its presence in a lipid bilayer does influence one of the less well characterized physical parameters associated to biological membranes: the membrane dipole potential. The importance of this electrostatic potential is only recently becoming apparent in relation to some biological processes (*27*−*35*). In the case of fusion peptides, it has been previously described that variations in

the magnitude of the dipole potential do affect the extension of the membrane fusion process triggered by a 12 residue long peptide from the simian immunodeficiency virus (*37*). In the present work, we undertook a more systematic study in order to determine which effects caused by cholesterol on peptide−membrane interactions can be assigned either to variations in the magnitude of the dipole potential or to changes in other membrane parameters such as the level of hydration and membrane fluidity. The main objective was to study the influence of cholesterol in each one of the different peptide−membrane interaction events which have been kinetically described previously in Buzón et al. (*16*): membrane binding followed by a conformational change (transformation of helical plus unordered structures into β-aggregates) which precedes lipid mixing. In order to distinguish the influence of the membrane dipole potential from the influence of hydration and membrane fluidity, we have used cholesterol and 6-ketocholestanol as components of the model membranes described in Figure 1. Both compounds are known to increase the magnitude (making it more positive toward the center of the lipid bilayer) of the membrane dipole potential (Figure 1B and refs *42* and *45*). Cholesterol, however, increases the hydration of the lipid headgroups in the lipid bilayer (Figure 7) and decreases membrane fluidity, whereas 6-ketocholestanol reduces membrane hydration (Figure 7) and increases membrane fluidity (*53*).

Our data show that an increase in the magnitude of the dipole potential (by adding either cholesterol or 6-ketocholestanol to the membranes) does reduce the dissociation constant of the binding process; that is, the affinity of the peptide for the membrane increases (Figures 2 and 3). This means that when the peptide potential is higher, a lower peptide concentration is required in order to fill a given percentage of the total number of possible "binding sites". Dipole potential does not seem to affect, however, the conformational transition (transformation of helical plus unordered structures into β-aggregates) that follows membrane binding (Figure 6). Mole percentages of either cholesterol or 6-ketocholestanol causing an equivalent increase in the magnitude of the dipole potential (the same ratio R in Figure 1B) affect differently the conformational transition. The increase in the amount of β-aggregates formed in the presence of 15 mol % 6-ketocholestanol and the lack of effect observed when there is 50 mol % cholesterol in the membranes must be related to the opposite influence of these compounds on membrane fluidity or hydration. Finally, both the extent and the kinetics of the lipid mixing process are affected by the presence of cholesterol and 6-ketocholestanol in the model membranes (Figure 4). It can be deduced that the increase in the magnitude of the dipole potential caused by either 6-ketocholestanol (15 and 30 mol %) or cholesterol (40 mol %) does increase the lipid mixing rate (Figure 4A,B). In the case of cholesterol, however, if we further increase its membrane content to 50 mol %, the effect on the lipid mixing rate seems to be reverted, getting back to the initial lipid mixing rate measured for the control (PC/PE membrane). The effect of cholesterol on the lipid mixing rate seems to have an optimum; once this optimum is exceeded, other physical properties, such as membrane fluidity, may be taking over, balancing and finally overcoming the dipole poential effect. Lipid mixing extent, however, seems to depend on parameters such as hydration and/or membrane fluidity, since 6-ketocholestanol increases lipid mixing whereas cholesterol decreases it.

In conclusion, it is clear from our results that part of the importance of the presence of cholesterol in the HIV envelope membrane can be due to its influence on the magnitude of the membrane dipole potential. We have shown that an increase in the magnitude of this electrostatic potential can increase the affinity of the fusion peptide for the membrane and the lipid mixing rate. Other events in the membrane fusion process (conformational transitions, lipid mixing extent) seem to be dependent on other membrane parameters, such as membrane hydration and fluidity.

ACKNOWLEDGMENT

We are grateful to Dr. Tzvetana Lazarova for reading the manuscript and for valuable suggestions.

REFERENCES

1. Eckert, D. M., and Kim, P. S. (2001) Mechanisms of viral membrane fusion and its inhibition, *Annu. Rev. Biochem. 70*, 777−810.
2. Peisajovich, S. G., and Shai, Y. (2002) New insights into the mechanism of virus-induced membrane fusion, *Trends Biochem. Sci. 27*, 183−190.
3. Veronese, F. D., DeVico, A. L., Copeland, T. D., Oroszlan, S., Gallo, R. C., and Sarngadharan, M. G. (1985) Characterization of gp41 as the transmembrane protein coded by the HTLV-III/LAV envelope gene, *Science 229*, 1402−1405.
4. Center, R. J., Leapman, R. D., Lebowitz, J., Arthur, L. O., Earl, P. L., and Moss, B. (2002) Oligomeric structure of the human immunodeficiency virus type 1 envelope protein on the virion surface, *J. Virol. 76*, 7863−7867.
5. Clapham, P. R., Reeves, J. D., Simmons, G., Dejucq, N., Hibbitts, S., and McKnight, A. (1999) HIV coreceptors, cell tropism and inhibition by chemokine receptor ligands, *Mol. Membr. Biol. 16*, 49−55.
6. Gallo, S. A., Finnegan, C. M., Viard, M., Raviv, Y., Dimitrov, A., Rawat, S. S., Puri, A., Durell, S., and Blumenthal, R. (2003) The HIV Env-mediated fusion reaction, *Biochim. Biophys. Acta 1614*, 36−50.
7. Tamm, L. K., and Han, X. (2000) Viral fusion peptides: a tool set to disrupt and connect biological membranes, *Biosci. Rep. 20*, 501−518.
8. Freed, E. O., Myers, D. J., and Risser, R. (1990) Characterization of the fusion domain of the human immunodeficiency virus type 1 envelope glycoprotein gp41, *Proc. Natl. Acad. Sci. U.S.A. 87*, 4650−4654.
9. Freed, E. O., Delwart, E. L., Buchschacher, G. L., Jr., and Panganiban, A. T. (1992) A mutation in the human immunodeficiency virus type 1 transmembrane glycoprotein gp41 dominantly interferes with fusion and infectivity, *Proc. Natl. Acad. Sci. U.S.A. 89*, 70−74.
10. Delahunty, M. D., Rhee, I., Freed, E. O., and Bonifacino, J. S. (1996) Mutational analysis of the fusion peptide of the human immunodeficiency virus type 1: identification of critical glycine residues, *Virology 218*, 94−102.
11. Bosch, M. L., Earl, P. L., Fargnoli, K., Picciafuoco, S., Giombini, F., Wong-Staal, F., and Franchini, G. (1989) Identification of the fusion peptide of primate immunodeficiency viruses, *Science 244*, 694−697.
12. Chan, D. C., Fass, D., Berger, J. M., and Kim, P. S. (1997) Core structure of gp41 from the HIV envelope glycoprotein, *Cell 89*, 263−273.
13. Tan, K., Liu, J., Wang, J., Shen, S., and Lu, M. (1997) Atomic structure of a thermostable subdomain of HIV-1 gp41, *Proc. Natl. Acad. Sci. U.S.A. 94*, 12303−12308.
14. Weissenhorn, W., Dessen, A., Harrison, S. C., Skehel, J. J., and Wiley, D. C. (1997) Atomic structure of the ectodomain from HIV-1 gp41, *Nature 387*, 426−430.
15. Rafalski, M., Lear, J. D., and DeGrado, W. F. (1990) Phospholipid interactions of synthetic peptides representing the N-terminus of HIV gp41, *Biochemistry 29*, 7917−7922.

16. Buzon, V., Padros, E., and Cladera, J. (2005) Interaction of fusion peptides from HIV gp41 with membranes: a time-resolved membrane binding, lipid mixing, and structural study, *Biochemistry 44*, 13354−13364.
17. Sackett, K., and Shai, Y. (2003) How structure correlates to function for membrane associated HIV-1 gp41 constructs corresponding to the N-terminal half of the ectodomain, *J. Mol. Biol. 333*, 47−58.
18. Sackett, K., and Shai, Y. (2005) The HIV fusion peptide adopts intermolecular parallel beta-sheet structure in membranes when stabilized by the adjacent N-terminal heptad repeat: A (13)C FTIR study, *J. Mol. Biol. 350*, 790−805.
19. Saez-Cirion, A., and Nieva, J. L. (2002) Conformational transitions of membrane-bound HIV-1 fusion peptide, *Biochim. Biophys. Acta 1564*, 57−65.
20. Yang, J., Gabrys, C. M., and Weliky, D. P. (2001) Solid-state nuclear magnetic resonance evidence for an extended beta strand conformation of the membrane-bound HIV-1 fusion peptide, *Biochemistry 40*, 8126−8137.
21. Yang, J., and Weliky, D. P. (2003) Solid-state nuclear magnetic resonance evidence for parallel and antiparallel strand arrangements in the membrane-associated HIV-1 fusion peptide, *Biochemistry 42*, 11879−11890.
22. Aloia, R. C., Jensen, F. C., Curtain, C. C., Mobley, P. W., and Gordon, L. M. (1988) Lipid composition and fluidity of the human immunodeficiency virus, *Proc. Natl. Acad. Sci. U.S.A. 85*, 900−904.
23. Aloia, R. C., Tian, H., and Jensen, F. C. (1993) Lipid composition and fluidity of the human immunodeficiency virus envelope and host cell plasma membranes, *Proc. Natl. Acad. Sci. U.S.A. 90*, 5181−5185.
24. Viard, M., Parolini, I., Sargiacomo, M., Fecchi, K., Ramoni, C., Ablan, S., Ruscetti, F. W., Wang, J. M., and Blumenthal, R. (2002) Role of cholesterol in human immunodeficiency virus type 1 envelope protein-mediated fusion with host cells, *J. Virol. 76*, 11584−11595.
25. Liao, Z., Cimakasky, L. M., Hampton, R., Nguyen, D. H., and Hildreth, J. E. (2001) Lipid rafts and HIV pathogenesis: host membrane cholesterol is required for infection by HIV type 1, *AIDS Res. Hum. Retroviruses 17*, 1009−1019.
26. Manes, S., del Real, G., Lacalle, R. A., Lucas, P., Gomez-Mouton, C., Sanchez-Palomino, S., Delgado, R., Alcami, J., Mira, E., and Martinez, A. C. (2000) Membrane raft microdomains mediate lateral assemblies required for HIV-1 infection, *EMBO Rep. 1*, 190−196.
27. Alakoskela, J. I., and Kinnunen, P. K. (2001) Control of a redox reaction on lipid bilayer surfaces by membrane dipole potential, *Biophys. J. 80*, 294−304.
28. Alakoskela, J. M., Soderlund, T., Holopainen, J. M., and Kinnunen, P. K. (2004) Dipole potential and head-group spacing are determinants for the membrane partitioning of pregnanolone, *Mol. Pharmacol. 66*, 161−168.
29. Antonenko, Y. N., Rokitskaya, T. I., and Kotova, E. A. (1999) Effect of dipole modifiers on the kinetics of sensitized photoinactivation of gramicidin channels in bilayer lipid membranes, *Membr. Cell Biol. 13*, 111−120.
30. Hristova, K., Dempsey, C. E., and White, S. H. (2001) Structure, location, and lipid perturbations of melittin at the membrane interface, *Biophys. J. 80*, 801−811.
31. Rokitskaya, T. I., Antonenko, Y. N., and Kotova, E. A. (1997) Effect of the dipole potential of a bilayer lipid membrane on gramicidin channel dissociation kinetics, *Biophys. J. 73*, 850−854.
32. Rokitskaya, T. I., Kotova, E. A., and Antonenko, Y. N. (2002) Membrane dipole potential modulates proton conductance through gramicidin channel: movement of negative ionic defects inside the channel, *Biophys. J. 82*, 865−873.
33. Schagina, L. V., Gurnev, P. A., Takemoto, J. Y., and Malev, V. V. (2003) Effective gating charge of ion channels induced by toxin syringomycin E in lipid bilayers, *Bioelectrochemistry 60*, 21−27.
34. Voglino, L., McIntosh, T. J., and Simon, S. A. (1998) Modulation of the binding of signal peptides to lipid bilayers by dipoles near the hydrocarbon-water interface, *Biochemistry 37*, 12241−12252.
35. Zhang, L., Rozek, A., and Hancock, R. E. (2001) Interaction of cationic antimicrobial peptides with model membranes, *J. Biol. Chem. 276*, 35714−35722.
36. Brockman, H. (1994) Dipole potential of lipid membranes, *Chem. Phys. Lipids 73*, 57−79.
37. Cladera, J., Martin, I., Ruysschaert, J. M., and O'Shea, P. (1999) Characterization of the sequence of interactions of the fusion domain of the simian immunodeficiency virus with membranes. Role of the membrane dipole potential, *J. Biol. Chem. 274*, 29951−19959.
38. Franklin, J. C., and Cafiso, D. S. (1993) Internal electrostatic potentials in bilayers: measuring and controlling dipole potentials in lipid vesicles, *Biophys. J. 65*, 289−299.
39. Simon, S. A., McIntosh, T. J., Magid, A. D., and Needham, D. (1992) Modulation of the interbilayer hydration pressure by the addition of dipoles at the hydrocarbon/water interface, *Biophys. J. 61*, 786−799.
40. Mayer, L. D., Hope, M. J., and Cullis, P. R. (1986) Vesicles of variable sizes produced by a rapid extrusion procedure, *Biochim. Biophys. Acta 858*, 161−168.
41. Golding, C., Senior, S., Wilson, M. T., and O'Shea, P. (1996) Time resolution of binding and membrane insertion of a mitochondrial signal peptide: correlation with structural changes and evidence for cooperativity, *Biochemistry 35*, 10931−10937.
42. Cladera, J., and O'Shea, P. (1998) Intramembrane molecular dipoles affect the membrane insertion and folding of a model amphiphilic peptide, *Biophys. J. 74*, 2434−2442.
43. Gross, E., Bedlack, R. S., Jr., and Loew, L. M. (1994) Dual-wavelength ratiometric fluorescence measurement of the membrane dipole potential, *Biophys. J. 67*, 208−216.
44. Struck, D. K., Hoekstra, D., and Pagano, R. E. (1981) Use of resonance energy transfer to monitor membrane fusion, *Biochemistry 20*, 4093−4099.
45. Asawakarn, T., Cladera, J., and O'Shea, P. (2001) Effects of the membrane dipole potential on the interaction of saquinavir with phospholipid membranes and plasma membrane receptors of Caco-2 cells, *J. Biol. Chem. 276*, 38457−38463.
46. Clarke, R. J. (1997) Effect of lipid structure on the dipole potential of phosphatidylcholine bilayers, *Biochim. Biophys. Acta 1327*, 269−278.
47. Byler, D. M., and Susi, H. (1986) Examination of the secondary structure of proteins by deconvolved FTIR spectra, *Biopolymers 25*, 469−487.
48. Blume, A., Hubner, W., and Messner, G. (1988) Fourier transform infrared spectroscopy of $^{13}C{=}O$-labeled phospholipids hydrogen bonding to carbonyl groups, *Biochemistry 27*, 8239−8249.
49. Mantsch, H. H., and McElhaney, R. N. (1991) Phospholipid phase transitions in model and biological membranes as studied by infrared spectroscopy, *Chem. Phys. Lipids 57*, 213−226.
50. Schaffner, C. P., Plescia, O. J., Pontani, D., Sun, D., Thornton, A., Pandey, R. C., and Sarin, P. S. (1986) Anti-viral activity of amphotericin B methyl ester: inhibition of HTLV-III replication in cell culture, *Biochem. Pharmacol. 35*, 4110−4113.
51. Reimund, E. (1986) Envelope perturbation and AIDS, *Lancet 2*, 1159.
52. Sarin, P. S., Gallo, R. C., Scheer, D. I., Crews, F., and Lippa, A. S. (1985) Effects of a novel compound (AL 721) on HTLV-III infectivity in vitro, *N. Engl. J. Med. 313*, 1289−1290.
53. Auner, B. G., O'Neill, M. A., Valenta, C., and Hadgraft, J. (2005) Interaction of phloretin and 6-ketocholestanol with DPPC-liposomes as phospholipid model membranes, *Int. J. Pharmacol. 294*, 149−155.

BI060622I